Plant Ecology and Evolution 143 (3): 297–306, 2010
doi:10.5091/plecevo.2010.415

REGULAR PAPER

Discrete free-boundary reaction-diffusion model of diatom pore occlusions

Lisa Willis[1,2,4,*], Karen M. Page[1,2], David S. Broomhead[3] & Eileen J. Cox[4]

[1]CoMPLEX, University College London, Physics Building, Gower St, London, UK-WC1E 6BT, United Kingdom
[2]Department of Mathematics, University College London, Gower St, London, UK-WC1E 6BT, United Kingdom
[3]MIMS, The University of Manchester, School of Mathematics, Oxford Road, Manchester, UK-M13 9PL, United Kingdom
[4]Natural History Museum, Cromwell Road, London, UK-SW7 5BD, United Kingdom
*Author for correspondence: l.willis@ucl.ac.uk

Background – Diatoms are unicellular algae, prolific in nearly all aqueous environments on earth. They are encased between two siliceous valves that each feature a variety of intricately patterned species-specific siliceous structures. How diatoms use biological and physical processes to form these tiny detailed structures is largely unknown. This work is concerned with the smallest regular structures in diatom valves, the pore occlusions, and the processes involved in their formation.
Theory and method – We developed a discrete, free-boundary, reaction-diffusion computer model to assess a new physically motivated hypothesis: pore occlusion patterns in the genus *Achnanthes* are simply expressions of silica diffusion and deposition within a pore covered by a membrane (silicalemma), whose deformation interacts with the growth of the pore boundary to control the silica influx.
Preliminary results and discussion – Simulations generate some promising pore features such as bifurcating and curved protrusions that grow towards one another, as seen in diatom pore occlusions. But they tend to be irregular and, to date, taking into account of smoothing and regularizing effects only partially symmetrized formations. Potential future work on this point is outlined.

Key words – diatoms, valve morphogenesis, pore occlusions, discrete free-boundary reaction-diffusion model.

INTRODUCTION

Diatoms are unicellular algae, prolific in the world's waters, critical in food chains ascending to fish, and fundamental in the carbon cycle. The curious porous forms of their species-specific siliceous valves are a striking example of how a eukaryotic cell controls structure at a minute scale in a manner that defies synthesis *in vitro*. The variety of intricate patterns in valve morphogenesis is breathtaking. What physico-chemical and mechanical processes can generate such variety while retaining high genotypic fidelity? In this article we briefly review current evidence on the finest structures of diatom valves, the sub-micron patterns observed in their pore occlusions. We then describe our first attempts to test a new theoretical model of pore occlusion formation.

BACKGROUND

The formation of pore occlusions is usually the last stage of valve morphogenesis

Upon cytokinesis of a diatom cell, each daughter cell initiates the construction of an organelle which houses a newly forming valve within a lipid bilayer membrane 7 nm thick called the silicalemma (Drum & Pankratz 1964, Reimann et al. 1966). Electron microscope (EM) studies have established the following common series of events in valve morphogenesis (e.g. Pickett-Heaps et al. 1990, Schmid 1994).

Pore delimitation: early formation of the larger pores – Early on the valve grows laterally, primarily from its rim, while the silicalemma expands laterally to accommodate this

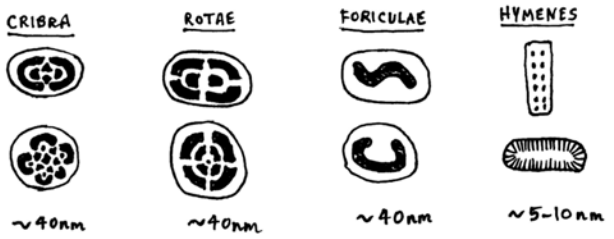

Figure 1 – Illustrations of types of pore occlusions. The perforations in cribra, rotae, and foriculae are approximately 40 nm across, while hymenes are distinguished by their tiny perforations 5–10 nm. Rotae have one or more bars on their axes. Foriculae have a single, simply connected perforation.

growth. Silica precursors, derived ultimately from soluble monosilicic acid $Si(OH)_4$ in the ocean (Del Amo & Brzezinski 1999), precipitate to form a delicate base-layer (a network of tessellated hexagons, or radial ribs (costae) with cross-connections, or parallel ribs (virgae) with cross-connections (vimines)), which gradually thickens and becomes more regular delimiting a regular arrangement of well-defined pores (areolae) 200–900 nm in diameter (e.g. Round et al. 1990). Soon after precipitation, the solid biogenic silica appears as a collection of loosely aggregated small nanospheres 20–50 nm diameter (Schmid 1976, Chiappino & Volcani 1977, Schmid 1979, Cox 1999: figs 5–12). Over time, the aggregations gradually condense and acquire a smooth appearance in the SEM[1]. The solid hydrated silica SiO_2 of the valve appears to be amorphous in most species even on the atomic scale (Vrieling et al. 2000, 2003), so crystal nucleation and directed crystal growth do not feature in morphogenesis. Although in *Pinnularia viridis* (Nitzsch) Ehrenb. at least, early silica deposition is directed by silica microfibrils parallel to one another and perpendicular to the valve's surface (Crawford et al. 2009).

Pore completion: nanofabrication of the pores creates the pore occlusions – Silica is nanofabricated within the delimited pores to form fine perforations 3–50 nm in diameter depending on species. These are the pore occlusions, classified by their final pattern as cribra (e.g. *Achnanthes coarctata* (Bréb.) Grunow, Cox 2004: figs 1, 2), rotae (e.g. *Rhaphoneis amphiceros* (Ehrenb.) Ehrenb., Cox 2004: figs 3, 4), foriculae (e.g. *Cymbella* s. lat. and *Gomphonema*, Cox 2004: figs 7–14), or hymenes (e.g. *Amphipleura* Kütz., *Berkeleya* Grev., Cox 1975: figs 13, 15–17) (Cox 1975, Ross et al. 1979, Mann 1981, Cox 2004), as illustrated in fig. 1.

In every diatom each pore occlusion shares a characteristic pattern that is conserved within species, yet this submicron pattern varies considerably between species; some occlusion types are restricted to particular higher taxa, e.g. hymenes are only found within the raphid diatoms. So areola type can be systematically informative, and pore occlusion formation is somehow genetically regulated. What is the nature of this genetic regulation? As briefly discussed below, a convincing physical model of pore occlusion formation could provide some clue.

The functional role of pore occlusions is entirely unknown. In supplementary material we present a mathematical argument related to their functional role. It suggests that even if diffusion of nutrients is obstructed by solid silica components of the valve, provided that nutrients are frequently absorbed when they collide with the plasmalemma, the pores and the pore occlusions probably reduce the rate of nutrient-uptake into the cell by a surprisingly small factor considerably less than 50%, even though pore occlusion openings or perforations occupy only a small fraction of the valve's surface area, usually about 5 to 20%.

Evidence pertaining to pore occlusion formation

The form of biogenic silica precursors in the silicalemma is unknown – Inside the cell but outside the silicalemma, silica concentrations range from 19 to 340 mM depending on species (for review, see Martin-Jézéquel et al. 2000). Soluble silica saturates at a much lower concentration of 2mM for pHs below 9 (Iler 1979), so the cell is presumably packaging the silica with some stabilizing organic agent, otherwise silica would rapidly polymerize to form large colloids (Iler 1979) that, according to Martin-Jézéquel et al. (2000), are disruptive to the cell membrane[2]. Transportation of silica from within the cell to the silicalemma is thought to occur either by simple diffusion of organic ionophore-mediated mono- or polysilicic acid (Bhattacharyya & Volcani 1983), or actively by transport vesicles containing organic stabilizing agents (Schmid & Schulz 1979). But, how the cell maintains precondensed silica in a supersaturated state and in what form biogenic silica precursors arrive at and diffuse within the silicalemma remains a mystery. Silica precursors within the silicalemma could be monosilicic acid (≈ 0.3 nm diameter), polymerized silicic acid (0.5–5 nm diameter, Iler 1979), or larger organo-silica complexes.

EM images suggest the valve pattern is moulded by a finely orchestrated set of components in the cytoplasm – SEM and TEM observations of intracellular events during valve morphogenesis led Schmid (1994 and references therein) to postulate that the primary features of the valve, such as pores, are moulded by cell-orchestrated components in the cytoplasm. According to Schmid (1994) approximately 200–1000 nm diameter vesicles are sandwiched tightly between the silicalemma and the plasmalemma in a manner that interferes with the growth of the silicalemma: they border the rim of the advancing silicalemma so as to mould the pores. Pore completion is initiated by the detachment of vesicles from the plasmalemma. Schmid called these vesicles 'spacer vesicles' and had earlier postulated that they contain biogenic silica precursors for silica deposition (Schmid & Schulz 1979, Sullivan 1986). For *Coscinodiscus wailesii* Gran & Angst, Schmid reported that endoplasmic reticulum vesicles appear

1 AFM studies have further revealed that in many species completed valves contain a variety of silica building blocks, from nanospheres 30–50 nm diameter, to smooth, texture-less, silica surfaces (Hildebrand et al. 2008).

2 There is evidence for such an organic agent (Werner 1966, Azam et al. 1974).

to mould the cribra. Monolayer lipid vesicles can be as small as 20 nm in diameter.

What is missing from this description is a physical explanation for the robust symmetric patterning of the valves. It seems likely that to generate this patterning efficiently, the cell has adopted and tuned some general physico-chemical principles.

An organic matrix may template silica deposition – The organelle of valve morphogenesis has not been isolated, and little is known of its contents. However, we do know that the silicalemma contains an aqueous mixture of silica precursors, free H+ ions (as the intralumenal pH is acidic, Vrieling et al. 1999), and a variety of organic components that have been discovered embedded within the siliceous valve.

The organic components include silaffins and silacidin peptides (Nakajima & Volcani 1969, Nakajima & Volcani 1970, Kröger et al. 1999, Poulsen & Kröger 2004, Wenz et al. 2008), and amphiphilic species-specific long-chain polyamines (Kröger et al. 2000, Sumper et al. 2005, Sumper & Brunner 2006, Sumper & Lehmann 2006). These interact with one another and the silica precursors and, it is postulated, organize themselves spontaneously into an energetically favourable two-phase template for silica deposition (of the pores at least; Sumper 2002, Lenoci & Camp 2008). One phase contains organic matter preventing silica deposition, the other phase is an aqueous template for silica deposition. Indeed, pioneering studies show that solutions of long-chain polyamines, silaffin peptides, and monosilicic acid precipitate in a disordered, yet approximately hexagonal pattern *in vitro*, reminiscent of the base-layer in some species. However, there is no direct evidence for templating by organic molecules at the tiny-scale of the pore occlusions, or that such a process could form the other, more intricate, structures of the valve.

The composition of the silicalemma may affect valve morphogenesis – Lipids and proteins often move fluidly on membranes, transiently self-organising into clusters, so it is feasible that deformations of the silicalemma cause the redistribution of its transport proteins in a manner that contributes to valve morphogenesis. Silicalemma deformations may be purely mechanical or due to the recruitment of new lipids. Grachev et al. (2008) postulated that the movement of aquaporins (membrane-bound proteins that mediate the transport of water; Kozono et al. 2002, de Groot & Grubmüller 2005) on the silicalemma gives rise to patterned precipitation of silica. Other candidates for membrane-bound proteins that contribute to valve morphogenesis are silica uptake transporters: a repertoire of monosilicic acid uptake transporters reside on the plasmalemma of the diatom cell, and are likely also to reside on the silicalemma since, upon completion of the valve, the silicalemma is presumed to fuse with the plasmalemma (for review, see Pickett-Heaps et al. 1990). Whether silicon transporters modulate the intralumenal silica concentration of the silicalemma relative to the cell is unknown.

THEORY AND METHOD

A host of biological factors may influence pore occlusion formation. The only factors that are almost certainly present as pores are completed are the solid silica base-layer of the valve, biogenic silica precursors, the aqueous medium that surrounds them, and the deformable silicalemma. Our starting point was to consider possible physico-chemical relationships between these factors. We describe a theoretical process that is being assessed by a computer model.

Hypothesis: pore occlusions are simply expressions of silica diffusion and deposition within a deformable silicalemma that couples silica deposition to silica influx

The central idea is that there is a natural coupling between the locations where biogenic silica precursors enter the forming pore occlusion, and the locations on the 'pore boundary' where inward growth takes place. The silicalemma can be envisaged as a deformable membrane sandwiching a solid periodic framework, which represents a base-layer at pore delimitation stage of valve morphogenesis. The mechanical and chemical configuration of the deformable membrane influences where biogenic silica precursors enter the forming pore. (This could happen in several ways; for example, if silicon transporters span the silicalemma, they may move to the flattest region of a bendy membrane where there is least curvature, or their conformations may alter in response to membrane tension.) Points on the pore boundary close to regions where the diffusing biogenic silica precursors entered

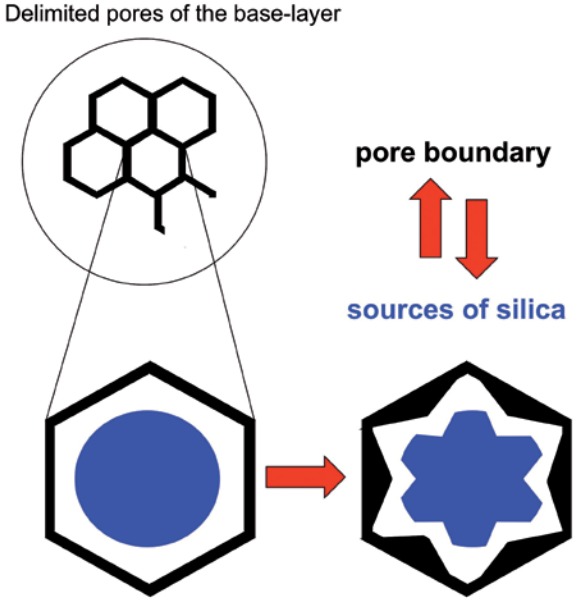

Figure 2 – Deposition of silica precursors alters the shape and size of the inward-growing delimited pores in the base-layer (the 'pore boundary', coloured black in the diagram) and this, in turn, alters where silica precursors enter the pore interior (the 'sources of silica', coloured blue in the diagram) so that different regions of the pore boundary thicken at different rates. The initial shape of the delimited pores may be a hexagon, or an ellipse, or a rectangle.

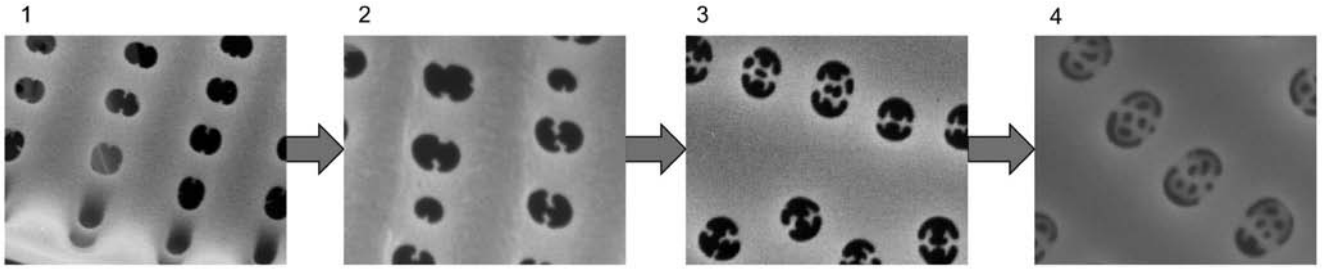

Figure 3 – SEM micrographs of partially formed pore occlusions of *Achnanthes coarctata* showing a possible time sequence 1–4 of their formation.

the pore will tend to accumulate precipitating silica more rapidly; inward growth will occur more rapidly here. Inward growth of the pore boundary alters the framework which the membrane sandwiches, which, in turn, alters the configuration of the membrane, and this may alter the region where silica enters the pore (fig. 2; silica entry is called 'silica influx'; the points where silica enters are called the 'sources' of the silica). In this way, silica deposition and silica influx are coupled via deformations of the silicalemma.

Discrete free-boundary reaction-diffusion model of pore occlusion formation

Mathematically this process could be modeled as a free-boundary reaction-diffusion continuum process (Appendix). This continuum model should give smooth inward growth of the pore boundary, yet as a model of the formation of pore occlusions it would be close to the limit of applicability: the tiny scale of pore occlusions components (approximately 5–40 nm) approaches that of the diffusing silica particles themselves (i.e. if the polymerized silica is 1–5 nm in diameter) and we cannot necessarily assume that the random jostling of particles due to inter-particle collisions 'averages out' at our tiny scale of observation as we would in a continuum model. Our model should consider the interactions between silica precursors and other molecules of the aqueous mixture within the pore. So we used a discrete computer model that features wandering silica precursors subject to random jostling.

In the computer model, jostling biogenic silica precursors are represented by random walkers on a square lattice of $l \times l$ sites. l is a dimensionless parameter related to the physical quantity L nm, the length of major axis of a delimited pore, and the unphysical quantity h nm, the resolution scale of observations, by $l = L/h$. Initially the pore boundary is a closed curve of lattice sites that matches the shape of the incipient delimited pores of the base-layer: the lattice approximation to an ellipse, hexagon, or rectangle. Random walkers, interior to the boundary, step to neighbouring non-boundary sites at rate D_0/h^2 without any particular bias. This represents diffusion of silica precursors with diffusivity D_0, where the physical quantity D_0 will depend on the size of the silica precursor and the viscosity of the aqueous mixture. Random walkers at sites adjacent to the boundary undergo precipitation reactions at rate $d_B k/h$, after which they can no longer diffuse. Once the volume of precipitated random walkers is sufficient to fill the volume of a particular lattice site, the boundary grows inward by this 1 lattice site. This represents deposition of silica precursors that precipitate at reaction rate k when they are within a binding distance d_B of the boundary. Upon deposition, a silica precursor advances the boundary inward by its precipitated volume v_B. Physical quantities d_B and k will depend on the type of chemical reaction, the structures of the reacting molecules, and the ionic composition of the aqueous mixture.

As described above, in order to simulate the possible effect of a deformable silicalemma upon silica influx, at any moment the shape of the pore boundary prescribes the location of the silica sources where random walkers enter the lattice and start their walk: the silica sources are always located at points in the pore interior that are farthest away from the boundary[3]. Importantly, this causes the sources of silica to move away from boundary protrusions and, in the absence of randomness (or the analogous continuum model), would give boundary growth with symmetry-planes that match the symmetry-planes of the delimited pore. The silica influx S_0, the number of new silica precursors that enter the pore per unit time, is a physical quantity that will depend on the mode of arrival of silica at the silicalemma.

Physical assumptions – Physical assumptions of this model are: the 3D dynamics within the pore are independent of the coordinate perpendicular to the plane of the base-layer, and can be approximated in 2D; dynamics can be represented on a square, anisotropic lattice; ions within the pore screen electrostatic interactions between silica precursors, and screen silica-precipitation reactions at the boundary unless precursors are within a given binding distance; silica influx is constant in time; the precipitation reaction at the boundary is independent of boundary curvature; and the only effect of the internal aqueous mixture is to agitate thermally the silica precursors (e.g. effects of volume-occupying inert polymers or vesicles are ignored).

PRELIMINARY RESULTS AND DISCUSSION

In all simulations, the initial shape of the pore boundary was chosen to match the delimited pores of *Achnanthes coarctata* (fig. 3): it is an ellipse with aspect ratio 4:3. Initially there are no silica precursors within the pore (this would be the

3 In the computer model this works as follows: at each lattice site in the pore interior, the smallest distance between that site and the boundary is calculated; then silica precursors enter at the sites where this distance is a maximum. If there are multiple sites, then silica precursors enter at each site with equal probability.

Table 1 – Parameters of the computer model for figs 4 & 5.

Parameter	Fig. 4						Fig. 5			
	A	B	C	D	E	F	A	B	C	D
'dimensionless silica influx' ($S_0 L^2/D_0$)	L^2	L^2	0.001 L^2	3.2 L^2	L^2	$2L^2$	L^2	L^2	3.2 L^2	8 L^2
'dimensionless precipitation reaction rate' ($k\, d_B L/ D_0$)	400 L	400 L	400 L	400 L	0.01 L	0.4 L	400 L	400 L	400 L	1000 L
'dimensionless volume of precipitated silica' (v_B/L^2)	$1/L^2$	$0.25/L^2$	$1/L^2$	$1/L^2$	$1/L^2$	$1/L^2$	$1/L^2$	$1/L^2$	$1/L^2$	$0.25/L^2$
volume occupation: 'dimensionless volume of silica in solution' (v_S/L^2)	-	-	-	-	-	-	$1/L^2$	-	-	$0.25/L^2$
resettling: 'resettling distance' (R_L/L), 'exposure' (E_L/L)	-	-	-	-	-	-	-	$4/L$, $3.5/L$	$4/L$, $3/L$	$6/L$, $5/L$

case if a spacer vesicle had been blocking the entry of silica). As pore occlusion patterns do not depend on time-scale or length-scale *per se*, only relative lengths and times need to be considered: the average time $1/(D_0/L^2)$ for a silica precursor to diffuse the initial diameter of the pore, compared with the average time $1/S_0$ between entries of new silica precursors and the average time $1/k$ for a precipitation reaction; the initial diameter of the pore L, compared with the binding distance d_B and the incremental distance moved by the boundary upon silica deposition $v_B^{1/2}$ (square root in 2D). These ratios give dimensionless parameters governing pore occlusion patterns: $S_0 L^2/D_0$ ('dimensionless silica influx'), $d_B k\, L/D_0$ ('dimensionless precipitation reaction rate'), and v_B/L^2 ('dimensionless volume of precipitated silica').

Parameters vary in the figures as indicated in table 1. Perturbations produce a few notable effects, outlined below. Reducing the unphysical parameter l ('number of lattice sites along each axis') improves computational efficiency. Ideally, perturbing l would not change statistical features of dynamics, but changes may originate from the anisotropy of the square lattice, or from the discretization of boundary movement. The effect of perturbing l is shown in fig. 4; in general, for $d_B k\, L/D_0 \gg 1$, reducing the ratio $l/(L/\sqrt{v_B})$ strengthens the effect of anisotropy (compare left column with right column in fig. 4A & B).

Slow silica influx $S_0 L^2/D_0 \approx 1$ symmetrizes pore boundary growth

As the dimensionless silica influx decreases to approximately one, dynamics of boundary growth becomes maximally sensitive to the silica deposition-silica influx coupling: as $S_0 L^2/D_0$ decreases, eventually the average time between the entry of a silica particle into the pore and its deposition is shorter than the average time between entries of different silica particles, and so every time silica enters the pore, boundary growth causes the sources of silica to move in response[4]. This symmetrizes pore boundary growth (compare fig. 4A & C); protrusions that form early on have less of a growth advantage, and the more uniform growth of several, more equally spaced protrusions is apparent, rather than growth of just 1–4 protrusions near the minor axis of the ellipse (fig. 4C). Rapid silica influx ($S_0 L^2/D_0 \gg 1$ – fig. 4D) concentrates silica densely near silica sources, forming one connected silica blob. The entire blob is rapidly invaded by the boundary when a protrusion reaches it. Our choice for how silica sources move in response to boundary growth seems to prevent opposing protrusions from meeting and joining unless silica influx is rapid.

Rapid precipitation reactions $d_B k\, L/D_0 \gg 1$ encourage growth of protrusions

When the dimensionless precipitation reaction rate is much greater than one, silica precursors aggregate to the boundary once they reach it: dynamics is 'diffusion-limited'. The resulting boundary structures, familiar from models of diffusion-limited-aggregation (Witten & Sander 1983), are too irregular to look like pore occlusions (fig. 4A–D). Reducing the dimensionless reaction rate to approach one (fig. 4E), silica is more uniformly distributed within the pore, so different sites on the pore boundary grow inward at more similar rates; this smoothes inward protruding bumps and fattens protruding fingers, but also reduces the effect of silica deposition-silica influx coupling (fig. 4E & F). If measured values of d_B, k, and D_0 in *Achnanthes* imply $d_B k\, L/D_0$ is close to one ($L \approx 200$ nm is known), then boundary dynamics is described as 'reaction-limited', and in this case our model cannot adequately explain pore occlusion formation.

The lower bound on the volume v_B/L^2 of precipitated silica seems to necessitate an additional physical explanation for boundary smoothness

The value of l (number of lattice sites along each axis) sets the resolution scale for observations. If $l = 1$, nothing is seen at all. If $l = L/\sqrt{v_B}$, dynamics are observed at the scale of individual precipitating silica particles, and boundary growth is bound to look somewhat jagged, as particles arrive at the boundary by diffusive random jostling. The only chance of seeing a regular, smooth boundary growth in this model is to

4 Decreasing $S_0 L^2/D_0$ far below one means that the pore is empty for long periods of time, and so further decreases in $S_0 L^2/D_0$ hardly alter statistical features of boundary growth, except for the time-scale.

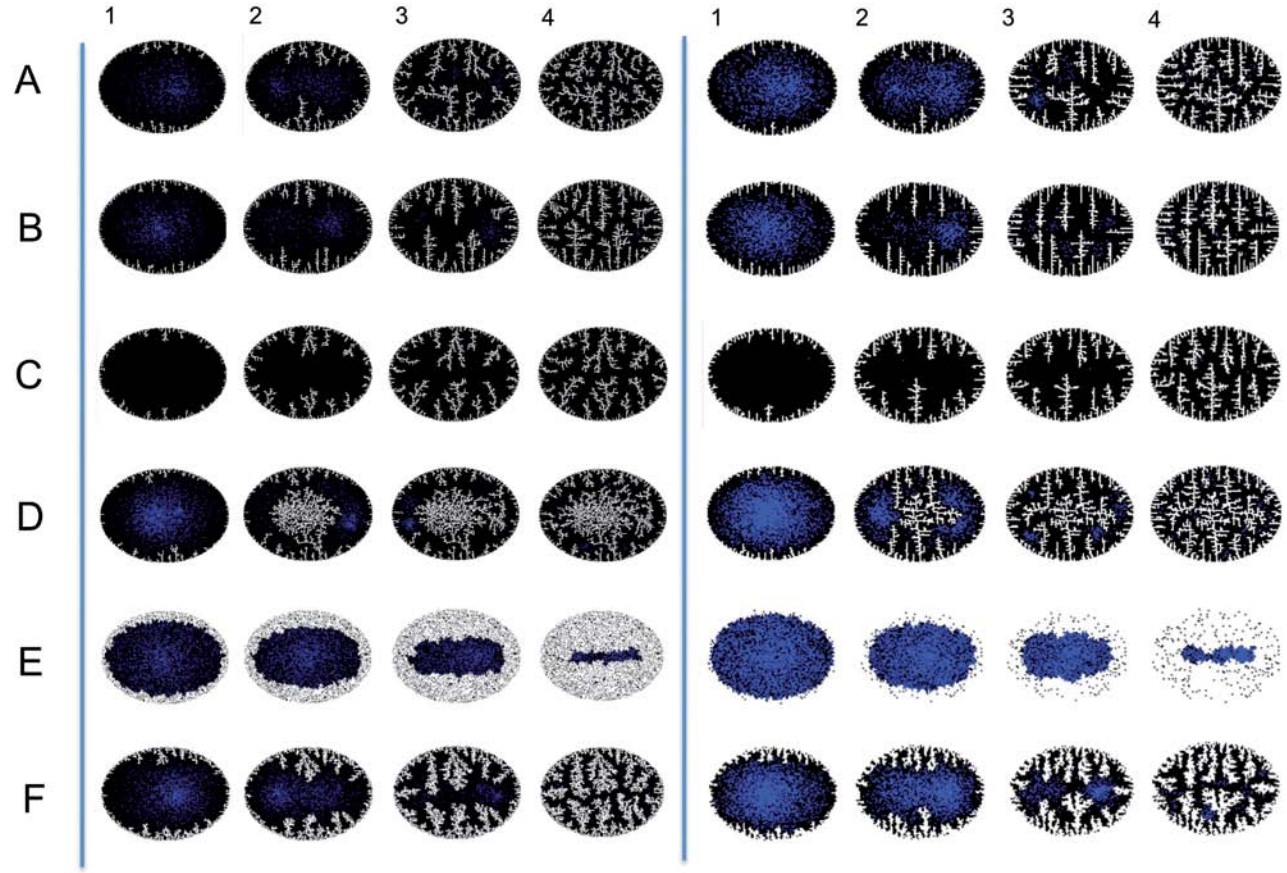

Figure 4 – Simulations of pore occlusions. Random walkers, coloured blue, represent biogenic silica precursors. The pore boundary is coloured white. Each row is a time series 1–4 for the parameters of table 1. In the left-hand column the scale $l = 200$; in the right-hand column $l = 100$. A: the simulation is too random and jagged compared to a pore occlusion. B: small volume of precipitated silica precursors – the smaller the ratio $l/(L/\sqrt{v_B})$, the stronger the effect of anisotropy. C: slow silica influx symmetrizes boundary growth. D: fast silica influx – boundary expands as one connected blob. E: slow precipitation reaction rate smoothes boundary and eliminates protrusions. F: intermediate precipitation reaction rate.

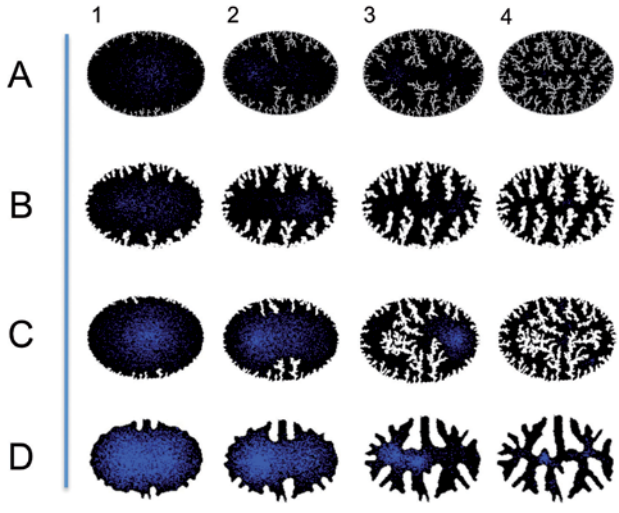

Figure 5 – Simulations showing the effects of volume-occupation and resettling. A: volume-occupation symmetrizes boundary growth. B–D: resettling helps protrusions to grow with a uniform thickness. Parameters are in table 1.

observe dynamics at a resolution scale determined by l where $1 \ll l \ll L/\sqrt{v_B}$. As the initial diameter of the pore $L \approx 200$ nm, the lower bound on the diameter of precipitated silica precursors of ≈ 0.2 nm (diameter of SiO_2) sets the maximum value of $L/\sqrt{v_B} \approx 200/0.2 = 1000$ and therefore the maximum range for l. For $L/\sqrt{v_B} = 1000$ and $l = 300 \ll L/\sqrt{v_B}$, in the diffusion-limited case, pore boundary growth is still random and jagged (results not shown). This and further simulations indicate that, in the diffusion-limited case, there is no physically plausible resolution scale that could account for smooth pore formation, so the model seems to require an additional physical explanation for this smoothness.

Factors that smooth and regularize pore formation

We investigated two physically motivated effects that smooth and regularize pore formation (computer algorithms detailed in Appendix).

Effect (1) is 'volume-occupation' of diffusing silica, dependent on the volume v_S of silica precursors in solution, it prevents silica precursors from entering or diffusing into lattice sites whose volume is already filled by silica. In the

results of fig. 4, silica precursors do not 'see one another' and the volume of silica in each lattice site is unlimited, an assumption that is invalid when silica precursors are concentrated (i.e. in the diffusion-limited case, when $S_0 L^2/D_0 \gg 1$).

Effect (2) is 'resettling' of precipitated silica. This envisages recently deposited silica being knocked a short distance (the 'resettling length' R_L) into a more tightly packed configuration by molecules in the surrounding solution. In the computer model, silica precursors may step to neighbouring sites within a certain distance, which are also adjacent to the boundary, but less exposed to the solution in the pore lumen.

How effects (1) and (2) alter the model's dynamics is shown in fig. 5. These generate more promising dynamics (compare with Fig. 4): volume-occupation encourages symmetric growth (compare figs 4A & 5A); resettling over a short-range smoothes the boundary without eliminating protrusions, helping protrusions to grow with a uniform thickness (fig. 5B). But to date, these smoothing and regularizing effects are not sufficient to account for the smooth, connected patterns seen in *Achnanthes coarctata*. We see that resettling-parameters strongly affect boundary dynamics (compare figs 4A & 5B), so, in future, smoothing algorithms should be realized by physical derivations which express smoothing-parameters in terms of potentially measurable physical quantities.

Relating physical quantities to pore occlusion type

Dimensionless combinations of physical quantities S_0, D_0, d_B k, v_B, and the size and shape of the delimited pore, govern pore occlusion formation according to our model, and may be influenced by genetic change. A convincing physical model that robustly mimicked pore occlusion formation in *Achnanthes coarctata*, and also reproduced the variety of pore occlusions observed in other species, could lead to predictions about how the cell physically regulates pore occlusion patterns. For example, to a very rough approximation our model implies that reducing the precipitation reaction rate k should cause a shift from pore occlusions resembling cribra, to pore occlusions resembling foriculae (compare fig. 1 with fig. 4C & 4E). Such predictions may provide clues to the nature of genetic regulation.

CONCLUSION

This is the first computational study that aims to identify the primary processes that govern pore occlusion formation. Computer studies have previously been used to investigate the stage of pore delimitation in valve morphogenesis (Gordon & Drum 1994, Parkinson et al. 1999, Bentley et al. 2005, Lenoci & Camp 2008). The most closely related study is by Parkinson et al. who used diffusion-limited aggregation (a well-known 2D model of randomly jostling molecules which wander from infinity to an outward growing dendritic structure nucleated by some central seed – Witten & Sander 1981) to model the arrival of microtubule-guided silica precursors at the margin of an expanding silicalemma. Here random walkers wandered from a line source or a set of point sources a fixed distance beyond the rim of the incipient valve. Our model inverts this process: random walkers on the interior of a nucleating surface cause inward growth. By locating sources at points that are farthest from the inward growing pore boundary, an extra stabilizing mechanism that encourages symmetric growth was automatically included. Further, we investigated a precipitation reaction rate that controls whether the model is diffusion-limited or reaction-limited. Our simulations generated some promising dynamics, but as yet we have been unable to account for the smooth and regular deposition of randomly jostling particles of silica at such tiny scales, or for the topology of pore occlusion perforations that in our model must result from fusions of finger-like protrusions of solid silica.

Although firm conclusions require a more thorough investigation of perturbations to our model (such as investigations of other smoothing algorithms, of 3D and non-lattice based models), these preliminary results suggest that the proposed process omits some important physical effect which enables pore occlusions to form in a smooth and connected manner: our hypothesis should be revised. The following interesting observations will be used to guide these revisions. Pore occlusion patterns are often all aligned, usually in the direction of the major axis of the diatom. What causes this? Could it be an effect of anisotropic tension in the silicalemma? The size of areola when pore occlusions begin to form is remarkably uniform in most species. Is this due to the orchestrated removal of 'spacer' vesicles that prevented silica deposition, or could it be due to the destabilization of a spatially homogeneous solution within the pore as the length of the pore decreases? Finally, solid silica components and perforations of pore occlusions often have similar wave-like thicknesses. Is there a physical explanation for this? Revisions could include models of multiple chemical species within a delimited pore, possibly featuring a number of identical zwitterionic polymers that coprecipitate with silica so as to further enhance the silica influx-silica deposition coupling as proposed in this paper. Or models of polymers or tiny spacer vesicles, either within the silicalemma or pressed-up against its surface, that prevent silica deposition in the volumes they occupy (the mere presence of macromolecules can encourage nanometer-micron-scale organization through what are known as excluded volume forces).

The great advantage of exploring ideas with theoretical and computational models is that all forces influencing results are automatically controlled, which is difficult to achieve in the laboratory, and the effects of select forces can be investigated relatively quickly. This is also a disadvantage: proving biological statements by theoretical models alone is rarely possible, as only select forces are included in any idealized simulation. At extreme scales, physical reasoning can be used to say 'only forces X, Y, and Z are important', and we can be confident that our model is an accurate model of the real world. But at cellular scales, it is evolutionarily inevitable that for most phenomena many different forces may be involved. Theoretical and computer models of cellular processes are then not much use on their own, but are primary tools for comparing the consequences of hypotheses with data from the laboratory. This is what we aim to do ultimately with our model of pore occlusion formation.

SUPPLEMENTARY DATA

Supplementary data about influx of nutrient into a diatom cell (illustrated by a table and a figure) are available in pdf format at *Plant Ecology and Evolution*, Supplementary Data Site (http://www.ingentaconnect.com/content/botbel/plecevo/supp-data).

ACKNOWLEDGEMENTS

This work was supported by a PhD studentship from the Engineering and Physical Sciences Research Council, UK. L.W. is very grateful to Tom Duke for helpful discussions. We are grateful to two anonymous reviewers for thoughtful suggestions.

REFERENCES

Azam F., Hemmingsen B.B., Volcani B.E. (1974) Role of silicon in diatom metabolism. V. Silicic acid transport and metabolism in the heterotrophic diatom Nitzschia alba. Archives of Microbiology 97: 103–14.

Bentley K., Cox E.J., Bentley P.J. (2005) Nature's batik: a computer evolution model of diatom valve morphogenesis. Journal of Nanoscience and Nanotechnology 5(1): 25–34.

Berg H.C. (1983) Random Walks in Biology. Princeton, Princeton University Press.

Berg H.C., Purcell E.M. (1977) Physics of Chemoreception. Biophysical Journal 20:193–219.

Bhattacharya P., Volcani B.E. (1983) Isolation of silicate ionophore(s) from the apochlorotic marine diatom Nitzschia alba. Biochemical and Biophysical Research Communications 114: 365–372.

Chiappino M.L., Volcani B.E. (1977) Studies on the biochemistry and fine structure of silica shell formation in diatoms VII. Sequential cell wall development in the pennate Navicula pelliculosa. Protoplasma 93: 205–221.

Cox E.J. (1975) A reappraisal of the diatom genus Amphipleura Kütz. using light and electron microscopy. British Phycological Journal 10: 1–12.

Cox E.J. (1999) Variation in patterns of valve morphogenesis between representatives of six biraphid diatom genera (bacillariophyceae). Journal of Phycology 35: 1297–1312.

Cox E.J. (2004) Pore occlusions in raphid diatoms – a reassessment of their structure and terminology, with particular reference to members of the Cymbellales. Diatom 20: 33–46.

Crawford S.A., Chiovitti A., Pickett-Heaps J., Wetherbee R. (2009) Micromorphogenesis during diatom wall formation produces siliceous nanostructures with different properties. Journal of Phycology 45: 1353–1362.

de Groot B.L., Grubmüller H. (2005) The dynamics and energetics of water pemeation and proton exclusion in aquaporins. Current Opinion in Structural Biology 15:176–83.

Del Amo Y., Brzezinski M.A. (1999) The chemical form of dissolved Si taken up by marine diatoms. Journal of Phycology 35:1162–1170.

Drum R.W., Pancratz H.S. (1964) Post mitotic fine structure of Gomphonema parvulum. Journal of Ultrastructural Research 10: 217–23.

Erban R., Chapman S.J. (2009) Stochastic modeling of reaction-diffusion processes: algorithms for bimolecular reactions. Physical Biology 6(4): 046001.

Erban R., Chapman S.J., Maini P.K. (2007) A practical guide to stochastic simulations of reaction-diffusion processes. Web resource available at: http://people.maths.ox.ac.uk/erban/Education/StochReacDiff.pdf

Gordon R., Drum R.W. (1994) The chemical basis for diatom morphogenesis. International Review of Cytology 150: 243–372.

Grachev M.A., Annenkov V.V., Likhoshway Y.V. (2008) Silicon nanotechnologies of pigmented heterokonts. BioEssays 30: 328–337.

Hildebrand M., Doktycz M.J., Allison D.P. (2008) Application of AFM in understanding biomineral formation in diatoms. European Journal of Physiology 456: 127–137.

Iler R.K. (1979) The chemistry of silica: Solubility, polymerization, colloid and surface properties, and biochemistry. New York, John Wiley & Sons, Inc.

Kozono D., Yasui M., King L.S., Agre P. (2002) Aquaporin water channels: atomic structure molecular dynamics meet clinical medicine. The Journal of Clinical Investigation 109: 1395–1399.

Kröger N., Deutzmann R., Sumper M. (1999) Polycationic peptides from diatom biosilica that direct silica nanosphere formation. Science 286: 1129–1132.

Kröger N., Deutzmann R., Bergsdorf C., Sumper M. (2000) Species-specific polyamines from diatoms control silica morphology. Proceedings of the National Academy of Sciences, U.S.A. 97: 14133–14138.

Lenoci L., Camp P.J. (2008) Diatom structures templated by phase-separation fluids. Langmuir 24: 217–223.

Mann D.G. (1981) Sieves and flaps: siliceous minutiae in the pores of raphid diatoms. In: Ross R. (ed) Proceedings of the 6th Symposium on recent and fossil diatoms. Budapest, 1980: 279–300. Koenigstein, Koeltz.

Martin-Jézéquel V., Hildebrand M., Brzezinski M.A. (2000) Silicon metabolism in diatoms: implications for growth. Journal of Phycology 36: 821–840.

Nakajima T., Volcani B.E. (1969) 3,4-Dihydroxyproline – a new amino acid in diatom cell wall. Science 164: 1400–1401.

Nakajima T., Volcani B.E. (1970) Epsilon-N-triemethyl-L-delta-hydroxysine phosphate and its non-phosphorylated compound in diatom cell walls. Biochemical and Biophysical Research Communications 39: 28–33.

Parkinson J., Brechet Y., Gordon R. (1999) Centric diatom morphogenesis: a model based on a DLA algorithm investigating the potential role of microtubules. Biochimica et Biophysica Acta (BBA) – Molecular Cell Research 1452: 89–102.

Pickett-Heaps J., Schmid A.M., Edgar L.A. (1990) The cell biology of diatom valve formation. In: Round F.E., Chapman D.J. (eds) Progress in phycological research 7: 1–169. Bristol, Biopress Limited.

Poulsen N., Kröger N. (2004) Silica morphogenesis by alternative processing of silaffins in the diatom Thalassiosira pseudonana. The Journal of Biological Chemistry 279: 42993–42999.

Reimann B.E., Leivin J.C., Volcani B.E. (1966) Studies on biochemistry and fine structure of silica shell formation in diatoms. II. Structure of cell wall of Navicula pelliculosa (Bréb.) Hilse. Journal of Phycology 2: 74–84.

Ross R., Cox E.J., Karayeva N.I., Mann D.G., Paddock T.B., Simonsen R., et al. (1979) An amended terminology for the sili-

ceous components of the diatom cell. Nova Hedwigia, Beiheft 64: 513–533.

Round F.E., Crawford R.A., Mann D.G. (1990) Diatoms: biology and morphology of the genera. Cambridge, Cambridge University Press.

Schmid A.M. (1976) Morphologische und physiologische untersuchungen an Diatomeen des Neusiedlersees. II. Nova Hedwigia 28: 309–351.

Schmid A.M. (1979) The development of structure in the shells of diatoms. Beihefte zur Nova Hedwigia 64: 219–236.

Schmid A.M. (1994) Aspects of morphogenesis and function of diatom cell-walls with implication for taxonomy. Protoplasma 181: 43–60.

Schmid A.M., Schulz D. (1979) Wall morphogenesis in diatoms: deposition of silica by cytoplasmic vesicles. Protoplasma 100: 267–288.

Sullivan C.W. (1986) Silicification by diatoms. Ciba Foundation Symposium 121:59–89.

Sumper M. (2002) A phase separation model for the nanopatterning of diatom biosilica. Science 295: 2430–2433.

Sumper M., Brunner E. (2006) Learning from diatoms: nature's tool for the production of nanostructured silica. Advanced Functional Materials 16: 17–26.

Sumper M., Brunner E., Lehmann G. (2005) Biomineralization in diatoms: characterization of novel polyamines associated with silica. FEBS Letters 579: 3765–3769.

Sumper M., Lehmann G. (2006) Silica pattern formation in diatoms: species-specific polyamine biosynthesis. ChemBioChem 9: 1419–1495.

Vrieling E.G., Beelen T.P., van Santen R.A., Gieskes W.W. (2000) Nanoscale uniformity of pore architecture in diatomaceous silica: a combined small and wide angle x-ray scattering study. Journal of Phycology 36: 146–159.

Vrieling E.G., Gieskes W.W., Beelen T.P. (1999) Silicon deposition in diatoms: control by the pH inside the silicon deposition vesicle. Journal of Phycology 35: 548–559.

Vrieling G.E., Hazelaar S., Gieskes W.W., Beelen T.P., Sun Q., et al. (2003) Silicon biomineralisation: towards mimicking biogenic silica formation in diatoms. Progress in Molecular and Subcellular Biology 33: 301–334.

Wenzl S., Hett R., Richthammer P., Sumper M. (2008) Silacidins: highly acidic phosphopeptides from diatom shells assist in silica precipitation in vitro. Angewandte Chemie International Edition 47: 1729–1732.

Werner D. (1966) Die Kieselsaure im Stoffwechsel von Cyclotella cryptica Reimann, Lewin und Guillard. Archiv für Mikrobiologie 55: 278–38.

Witten T.A., Sander L.M. (1981) Diffusion-limited aggregation, a kinetic critical phenomenon. Physical Review Letters 47(19): 1400–1403.

Paper based on results presented during the Symposium "Diatom Taxonomy in the 21st Century" (Meise 2009). Manuscript received 24 Dec. 2009; accepted in revised version 10 Jul. 2010.

Communicating Editor: Bart Van de Vijver.

Appendix – Free-boundary reaction-diffusion continuum model of pore occlusion formation and a probabilistic discrete analogue

This continuum model of the hypothesis features physical parameters that are potentially measurable. It helps us to write down an analogous discrete probabilistic computer model in terms of physical parameters. u($\mathbf{x}$,t) is the concentration of silica precursors at point $\mathbf{x}$ in the pore interior Ω at time t.

(1c) $\partial u(\mathbf{x},t)/\partial t = \nabla.(D\,\nabla u) + S/N\,\delta(\prod_i |\mathbf{x}-\mathbf{s}_i|)$ where $N = |\{\,\mathbf{s}_i\,\}|$ (see (5c)) (silica diffusion and entry into the pore);

(2c) $D = D_0,\ S = S_0$ (silica particles are small and dilute);
$D = D_0(1 - v_S\,u),\ S = S_0(1 - v_S\,u)$ (volume-occupying effect of silica);

(3c) $D\,\nabla u \,.\, \mathbf{n} = d_B\,k\,u$ in small volume at the boundary $\mathbf{x} : f(\mathbf{x},t) = 0$ (silica deposition);

(4c) $\partial f(\mathbf{x},t)/\partial t = -\,d_B\,k\,v_B\,u\,\nabla f \,.\, \mathbf{n}$ (boundary movement with normal speed $d_B\,k\,v_B\,u$);

(5c) $\{\mathbf{s}_i\} = \{\mathbf{z}: \mathbf{z}$ maximizes Euclidean distance from boundary$\}$; (silica sources' location);

(6c) $u(\mathbf{x},0) = g(\mathbf{x})$ and $f(\mathbf{x},0) = h(\mathbf{x}) = 0$ (initial distribution of silica and shape of pore boundary);

Parameters are described in the section Theory and Method.

Discrete probabilistic analogue used to simulate results – The following lattice-based discrete probabilistic analogue of the continuum model, implemented by the Gillespie Stochastic Simulation Algorithm (Erban et al. 2007, Erban & Chapman 2009), was used to produce results. This discrete model is analogous to the continuum model because upon taking appropriate limits

the time-evolution equations for the mean concentration of silica precursors are equivalent to continuum equations (1c-3c), and the mean normal speed of boundary growth is as in (4c).

Dynamics occur on a $d = 2$ dimensional cubic lattice of sites of length $h = L/l$. $\mathbf{x} = (x,y)$ denotes the site $[xh,(x+1)h] \times [yh, (y+1)h]$. The number of silica precursors or random walkers at site $\mathbf{x}$ within the pore interior Ω is $n_{\mathbf{x}}$. From site $\mathbf{x}$ random walkers may step to one of at most 4 adjacent sites $\mathbf{x} + \boldsymbol{\delta}$: $\boldsymbol{\delta} \in I = \{(0,1), (0, -1), (1,0), (-1,0)\}$. If $\mathbf{x} + \boldsymbol{\delta} \notin \Omega$ for some $\boldsymbol{\delta} \in I$, then $\mathbf{x}$ is adjacent to the pore boundary, denoted by $\mathbf{x} \in \partial\Omega$. The number of silica precursors that have precipitated at site $\mathbf{x}$ is denoted $b_{\mathbf{x}}$. In infinitesimal time Δt, a change in state occurs with the following transition probabilities up to $o(\Delta t)$:

(1d) $\mathbf{x} \in \Omega$, $\boldsymbol{\delta} \in I$, $\mathbf{x} + \boldsymbol{\delta} \in \Omega$: $(n_{\mathbf{x}}, n_{\mathbf{x}+\boldsymbol{\delta}}) \rightarrow (n_{\mathbf{x}}-1, n_{\mathbf{x}+\boldsymbol{\delta}}+1)$ prob. $n_{\mathbf{x}} D_0/h^2 \Delta t$ (silica diffusion)

(2d) $\mathbf{x} \in \{\mathbf{s}_i: i=1,.., N\}$: $n_{\mathbf{x}} \rightarrow n_{\mathbf{x}}+1$ prob. $S_0/N \Delta t$ (silica enters pore)

(3d) $\mathbf{x} \in \partial\Omega$: $(n_{\mathbf{x}}\, b_{\mathbf{x}}) \rightarrow (n_{\mathbf{x}}-1, b_{\mathbf{x}}+1)$ prob. $n_{\mathbf{x}} d_B k /h \ \Delta t$ (silica deposition)

where $\Omega \rightarrow \Omega\backslash\{\mathbf{x}\}$ and then $\{\mathbf{s}_i\} = \{\mathbf{z} \in \Omega$: $\mathbf{z}$ maximizes the Euclidean distance from $\mathbf{z}$ to $\partial\Omega\}$ are updated immediately whenever $b_{\mathbf{x}} \geq h^d/v_B$. The computer model is invalid when the resolution scale h is less than d_B or $v_B^{1/d}$.

In the results section, initially $n_{\mathbf{x}}=0$ and $b_{\mathbf{x}}= 0$ for all $\mathbf{x} \in \Omega$, and the set of sites within the pore $\mathbf{x} \in \partial\Omega$ form an ellipse of length L=200 nm, aspect ratio 4:3.

Algorithms for factors that smooth and regularize pore formation – To include the volume-occupying effect of silica precursors, the conditions of (1d) and (2d) are extended: (1d) $\mathbf{x} \in \Omega$, $\boldsymbol{\delta} \in I$, $\mathbf{x} + \boldsymbol{\delta} \in \Omega$, and $v_S n_{\mathbf{x}+\boldsymbol{\delta}} + v_B b_{\mathbf{x}+\boldsymbol{\delta}} < h^d$; (2d) $\mathbf{x} \in \{\mathbf{s}_i: i=1,..,N\}$, and $v_S n_{\mathbf{x}} + v_B b_{\mathbf{x}} < h^d$.

Upon deposition (event (3d)), silica may *resettle* locally at a nearby site that is also adjacent to the boundary within a dimensionless distance R_L/L of the original site, as follows. The *exposure* to the interior solution at site $\mathbf{z}$, dependent on dimensionless length parameter E_L/L, is $e(\mathbf{z}) = 1/(\sum_{\mathbf{u} \in E(\mathbf{z})} b_{\mathbf{u}}\, w_{\mathbf{u},\mathbf{z}})$, where $E(\mathbf{z}) = \{\mathbf{u} : \mathbf{u}$ belongs to the cube centered on $\mathbf{z}$ with sides of length ceiling$(E_L)\}$, and $w_{\mathbf{u},\mathbf{z}} = 1$ if $\mathbf{u}$ belongs to the cube centered on $\mathbf{z}$ with sides of length floor(E_L); otherwise $w_{\mathbf{u},\mathbf{z}} = E_L -$ floor(E_L). Precipitated silica resettles at the site within distance R_L/L to minimize exposure; it stays put if no site within distance R_L/L reduces exposure, and it moves with equal probability to sites that have equal, minimal exposure.